Proceedings of the 28th IEEE
EMBS Annual International Conference
New York City, USA, Aug 30-Sept 3, 2006

Hybrid Diffusion Imaging (HYDI)

Andrew L. Alexander, Yu-Chien Wu, and Pradeep C. Venkat

Abstract— **Hybrid diffusion imaging (HYDI) is a new diffusion MRI method for characterizing complex diffusion. Diffusion-weighted measurements are obtained on multiple 'shells' of constant diffusion weighting. This diffusion encoding approach is amenable to multiple types of diffusion imaging analysis. The inner shells may be used to estimate the diffusion tensor and generate maps of the diffusion anisotropy and mean diffusivity. The outer shell, which has high angular resolution, may be used to estimate the distribution of white matter fiber tracts in a voxel. Finally, all of the data may be used to estimate the diffusion displacement spectrum for characterizing the full diffusion behavior in a voxel. HYDI experiments were performed on the brains of healthy volunteers and the results are presented. Overall, HYDI is an efficient and promising method for characterizing complex diffusion in the human brain and potentially other tissues.**

I. Introduction

DIFFUSION MRI is a useful tool for the noninvasive study of microstructural architecture in the brain and other tissues. The diffusion tensor is a widely used and elegant model of water diffusion [1]. This model assumes that the diffusion displacements ($\mathbf{R} = \mathbf{R_1}-\mathbf{R_2}$) for a given diffusion time, Δ, may be described using Gaussian probability distribution,

$$P(\mathbf{R},\Delta) = \frac{1}{\sqrt{(4\pi\Delta)^3|\mathbf{D}|}} exp\left\{\frac{-\mathbf{R}^T\mathbf{D}^{-1}\mathbf{R}}{4\Delta}\right\} \quad (1)$$

which results in a mono-exponential decay with diffusion-weighting

$$S = S_o e^{-b\hat{\mathbf{g}}^T\mathbf{D}\hat{\mathbf{g}}} \quad (2)$$

where $\mathbf{D}$ is the diffusion tensor, $\hat{\mathbf{g}}$ is the unit vector describing the gradient orientation, S_o is the signal without diffusion weighting, and b is the amount of diffusion weighting.

At relatively low levels of diffusion-weighting (e.g., b < 1500 s/mm^2), the diffusion tensor is a good model of the diffusion-weighted signal behavior. However, the diffusion tensor model is often inaccurate for describing the signal behavior for higher levels of diffusion-weighting. The limitations with the simple diffusion tensor model arise from two primary causes – (i) a combination of apparent "fast" and "slow" diffusion [2,3] that cause non-monoexponential signal decay with diffusion-weighting (Fig 1); and (ii) partial volume averaging [4] between tissue groups with distinct diffusion tensor properties (e.g., intersecting white matter (WM) tracts, averaging between WM and gray matter tissues). The fast and slow diffusion signals are likely to arise from barriers caused by cellular membranes and compartmentalization of the water signals.

Partial volume effects cause ambiguities in the interpretation of diffusion tensor measurements. Diffusion anisotropy is generally assumed to be high in white matter; however, regions of crossing white matter tracts will have artifactually low diffusion anisotropy. Consequently, in areas with complex white matter organization, changes or differences in the diffusion tensor may reflect either changes in either the tissue microstructure or the partial volume averaging components. As the diffusion-weighting is increased, profiles of apparent diffusivity reveal non-Gaussian diffusion behavior in voxels with partial volume averaging.

In this paper, we describe a novel diffusion encoding method called hybrid diffusion imaging (HYDI), which obtains diffusion-weighted measurements at multiple levels (shells) of diffusion weighting with increasing angular resolution at higher diffusion-weighting. The method is amenable to different diffusion image analysis strategies. The inner shells may be processed using the diffusion tensor model. The outer shells provide the highest angular resolution for characterizing regions of crossing white matter fibers and is processed using q-ball imaging (QBI) approaches. The entire data set may be processed using Fourier q-space methods [5], which include diffusion spectrum imaging (DSI) [6].

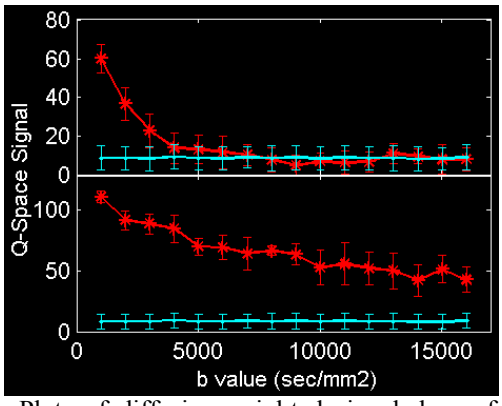

Fig 1. Plots of diffusion-weighted signal decay for grey matter (top) and white matter perpendicular to the WM fiber tracts (bottom). The white matter shows considerable signal (~40%) at very high diffusion-weighting (b=16,000s/mm^2).

Manuscript received May 15, 2006. This work was supported in part by the National Institute of Mental Health under Grant MH62015.

A. L. A. is with the Waisman Laboratory for Brain Imaging and Behavior, Departments of Medical Physics and Psychiatry, University of Wisconsin, Madison, WI 53705 USA (corresponding author; phone: 608-265-8233; fax: 608-262-9440; e-mail: alalaexander2@ wisc.edu).

Y-C. W and P. C. V. are both with the Waisman Laboratory for Brain Imaging and Behavior, University of Wisconsin, Madison, WI 53705 USA (e-mail: yuchienwu@wisc.edu, chilakamarri@wisc.edu).

II. Background

A. Diffusion Spectrum Imaging (DSI)

A growing number of strategies have been developed for measuring and interpreting complex diffusion behavior. The most basic approach for this application is diffusion spectrum imaging (DSI) [6] which uses diffusion-weighted samples on a Cartesian q-space lattice, where $\mathbf{q} = \gamma\mathbf{G}\delta$ is the diffusion-weighting wave-vector analogous to wave-vector $\mathbf{k}$ used in k-space sampling for MR image acquisitions. An excellent discussion of q-space imaging is found in the text by Callaghan [5]. For a specified diffusion time, Δ, the probability distribution of diffusion displacements, $P(\mathbf{R}, \Delta)$, is related to the distribution of sampled diffusion-weighted signals in q-space, $E(\mathbf{q}, \Delta)$, through a Fourier Transform:

$$P(\mathbf{R},\Delta) = \iiint E(\mathbf{q},\Delta)\, e^{-i2\pi\mathbf{q}\cdot\mathbf{R}}\, d^3\mathbf{q} \qquad (3)$$

The derivations of q-space formalism assume that the widths of the diffusion-pulses, δ, are narrow relative to the pulse spacing, Δ, such that $\delta << \Delta$. The maximum gradient amplitudes on current clinical MRI systems cause this assumption to be violated for diffusion spectrum imaging, since $\delta \sim \Delta$. The effect of this will be to slightly, but consistently underestimate the diffusion displacements, and the overall distribution shape will be correct [6]. Note that relationship of DSI (q-space) to diffusion tensor imaging is that $P(\mathbf{R},\Delta)$ is a multi-variate Gaussian (Equation (1)) and the diffusion-weighting factor is $b = |q|^2(\Delta-\delta/3)$ or $b \sim |q|^2\Delta$ for small δ. The DSI approach yields empirical estimates of the distributions of diffusion displacements (e.g., model free). Typically Cartesian q-space sampling is used for DSI. This is convenient from the Fourier analysis standpoint; however, it is extremely time consuming as each image represents only a single q-space measurement. The resolution of diffusion displacements (ΔR) is defined by the range of q-space samples: $\Delta R = \frac{1}{2}|q_{max}|$; and the alias-free range of displacements $2R_{max} = 1/\Delta q$. If the range of q-space samples is too small, then the measurement profile will be truncated, which will lead to Gibbs ringing in the reconstructed diffusion displacement spectrum. This can be ameliorated by apodization with a Hanning or Hamming window, at the cost of increased blurring of the diffusion distribution. Ideally the maximum $|q|$ should be large enough that the signal is near zero to minimize truncation effects. In adult white matter, this implies that a maximum diffusion weighting of 14,000 s/mm^2 or more is necessary although bmax ~ 10,000 s/mm^2 are probably reasonable. A common concern with very high diffusion-weighting is that the image SNR is very low. However, the Fourier transform associated with Equation (3) will improve the SNR by the square root of the number of samples (e.g., 400 DSI samples will improve the SNR of the displacement spectra by a factor of 20). Since the distributions of diffusion displacements are model independent, the distributions may be challenging to quantify. Several features have been proposed including the zero-displacement probability, $Po=P(\mathbf{R}=0,\Delta)$, which is higher in regions with more hindered or restricted diffusion; the mean squared displacement,

$$MSD(\Delta) = \iiint P(\mathbf{R},\Delta)\, |R|^2\, d^3\mathbf{R}, \qquad (4)$$

which is related to the diffusivity.

B. Q-Ball Imaging (QBI)

In order to better characterize the angular diffusion features associated with crossing white matter tracts, several diffusion encoding approaches have been developed that use a large number of encoding directions ($N_e > 40$ up to several hundred) at a fixed level of diffusion-weighting [7-10]. One approach is q-ball imaging (QBI) described by Tuch [11], which estimates the orientational distribution function (ODF) based upon the Funk-Radon Transform. According to this relationship, the ODF for a particular direction is equivalent to the circular integral about the equator perpendicular to the direction

$$ODF(\hat{\mathbf{r}}) = \int_{\mathbf{q}\perp\hat{\mathbf{r}}} E(\mathbf{q},\Delta)\, d^3\mathbf{q} \qquad (5)$$

This integral requires that the diffusivities be interpolated over the entire surface of the sphere. The peaks in the ODF profiles correspond to the specific WM tract directions. Since the ODF is estimated by integrating several measurements together, the SNR of the ODF will be much higher than that of the ADC values in the original apparent diffusion measurements.

C. Hybrid Diffusion Imaging (HYDI)

In this study, a new diffusion encoding strategy HYDI is described, which combines aspects of DTI, DSI and QBI. For DSI, while Cartesian sampling facilitates the straightforward FFT for estimation of the displacement densities, uniform Cartesian sampling is not required. In this study, q-space measurements are acquired on spherical shells of constant $|q|$ (diffusion-weighting). The angular resolution increases with the amount of diffusion-weighting. Diffusion-tensor analysis may be performed on the inner q-space shells (lower diffusion-weighting). Conversely, the outer shell with the highest diffusion-weighting may be configured to have the highest angular resolution for resolving crossing WM fiber tracts, and processed with QBI methods. Finally, the entire data set may be processed using diffusion-spectrum imaging (DSI) methods.

III. Methods

A. HYDI Acquisition

Hybrid diffusion imaging (HYDI) was performed on 20 healthy young adult volunteers. Informed consent was obtained from every subject in compliance with the guidelines of our Institutional Review Board. Images were acquired using a 3 Tesla whole body MRI scanner with an 8-channel receive-only head coil and maximum gradient amplitudes of 40 mT/m. Images were acquired using a single shot, pulsed-gradient spin echo pulse sequence with echo-planar readout and SENSE parallel imaging with a reduction factor of 2. The acquisition was gated using the pulse oximeter (TR = 10-15 heartbeats dependant upon heartrate); TE = 122 ms; FOV = 256 mm; matrix = 128x128

(interpolated to 256x256); and 30 contiguous axial 3 mm thick slices covering most of the cerebrum. The total acquisition time for 102 DW images for each slice was just under 30 minutes.

The diffusion encoding was performed using symmetric pulsed gradients with pulse width = 45 ms; and pulse spacing = 51 ms. The HYDI encoding scheme with 102 encoding directions is listed in Table I. There are six levels of diffusion-weighting and the q-space spacing is constant between shells. The field of view (FOV=$(2\Delta q_r)^{-1}$) and the resolution (max q_r^{-1}) of the displacement density of water molecular are 65 μm and 6.57 μm, respectively. The equivalent DSI sampling scheme with the same q-space sampling intervals and maximum radii (spherically apodized 11x11x11 Cartesian matrix) would require roughly 515 q-space images (albeit with overall higher angular resolution).

TABLE I. HYDI Encoding Scheme.

Shell	Dir. #	Δq_θ (°)	q_r (1/mm)	Δq_r (1/mm)	b value (sec/mm^2)
0	1				0
1	3		15.2	15.2	375
2	12	48°	30.4	15.2	1500
3	12	48°	45.6	15.2	3375
4	24	42°	60.9	15.2	6000
5	50	30°	76.0	15.2	9375
	Total 102	Mean 40°	Max 76.0	Mean 15.2	Max 9375

B. HYDI Processing

HYDI data were processed individually for each voxel. The inner 3 shells (0-2) were used to estimate the diffusion tensor and maps of mean diffusivity (MD) and fractional anisotropy (FA) were computed. White matter fiber orientations were estimated using QBI methods applied to the outer q-space shell with 50 directions. The orientation distribution function (ODF) was computed using Equation (5). The data from all shells were analyzed using DSI methods. First, measurements below an SNR of 2.5 were set to zero to minimize baseline noise effects. Trilinear interpolation was then used to interpolate the raw q-space data onto a Cartesian sampling grid and the displacement spectrum for each voxel was estimated using a 3D FFT (Equation 3). Convolution regridding methods are currently being investigated although they are not presented here. DSI maps of the zero-displacement probability (Po), mean squared displacement (MSD – Equation 4) and full width at half maximum (FWHM) in the X, Y and Z directions were computed.

IV. Results and Discussion

A. DTI and DSI Maps

An example of the DTI and DSI maps for one slice in one study are shown in Fig 2. The Po map from the DSI analysis has similar features to the FA map from the DTI analysis except that the value of Po is much more constant over all the WM. The zero-displacement probability Po is highest in regions of restricted diffusion such as in the direction perpendicular to the white matter fiber tracts. This method is relatively insensitive to regions of fiber crossings as it an integral of all the diffusion attenuation signals. In contrast, the FA map shows considerable heterogeneity in WM, because FA is highly sensitive to partial volume effects from crossing WM fibers. Thus Po may be a more specific marker of true changes in white matter microstructure. Recent work by Assaf et al. [12] suggest that Po is more consistent and sensitive than FA in multiple sclerosis. Maps of DTI MD and DSI MSD (theoretically proportional) are similar although there is more contrast between WM and grey matter (GM) in the MSD map. In this case, GM appears to have a decreased diffusivity relative to WM. Note that the DTI maps generally appear much noisier as the number of images used to generate them is significantly smaller (16 versus 102).

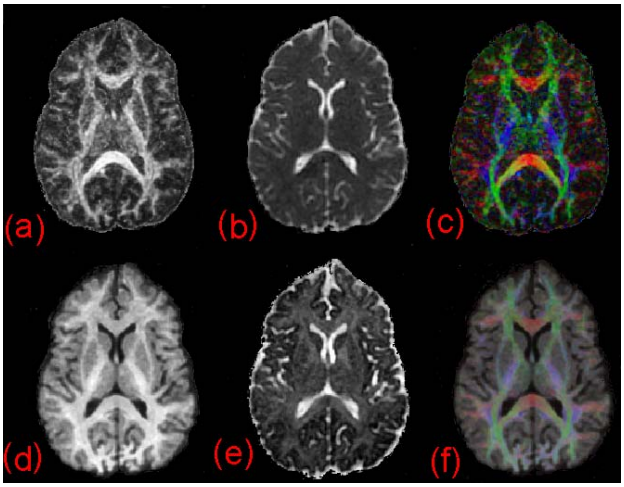

Fig 2. Comparison of DTI (top row) and DSI maps (bottom row) derived from the HYDI data set for a single slice. The DTI maps are (a) fractional anisotropy (FA), (b) mean diffusivity (MD), and (c) fiber orientation using the major eigenvector mapped onto color. The DSI maps are (d) the zero-displacement probability (Po), (e) mean squared displacement (MSD), and (f) the FWHM maps mapped into color channels, which highlight coherent WM orientation. The images in each column demonstrate interesting, but not identical features.

B. Non-monoexponential Diffusion

The diffusion tensor model assumes that the diffusion is Gaussian. As discussed earlier, the diffusion in brain tissues does not appear Gaussian when high diffusion-weighting is used. To examine this, the estimated diffusion tensors from the inner 3 shells were used to model the signal for the entire range of diffusion-weighting. Maps of the mean squared difference between the diffusion tensor model and measured signals were created and an example of the mean squared difference map is shown in Fig 3. This map shows that the

diffusion tensor model does not adequately describe diffusion attenuation behavior in white matter at high levels of diffusion-weighting.

C. *White Matter Fiber Architecture*

The orientation distribution function (ODF) was estimated using QBI methods applied to the outer shell of the HYDI data set. These method were able to reveal complex white matter organization in the brain stem at the level of the pons (Fig 4) and the centrum semiovale (Fig 5).

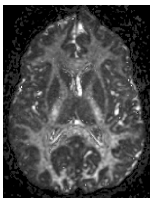

Fig 3. Map of mean squared difference between the signals predicted by the diffusion tensor model and the actual signals over the entire measured q-space. The difference is greatest in regions of white matter.

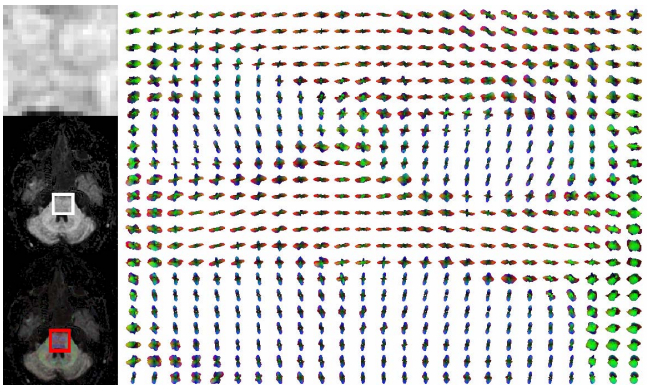

Fig 4. Maps of complex WM fiber organization at the cerebellar pontene level. Crossing fibers are observed at the intersection between WM tracts. Colors indicate direction: red (R/L); green (A/P); blue (S/I).

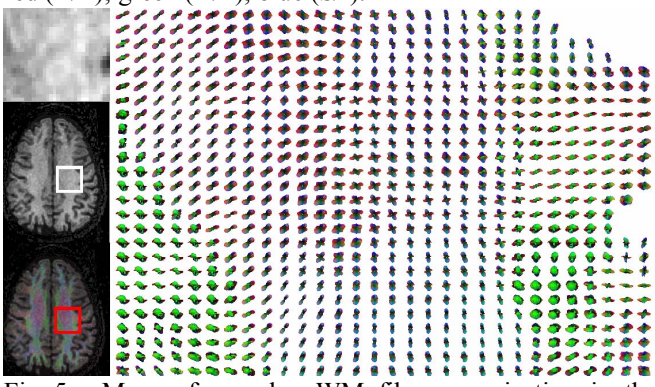

Fig 5. Maps of complex WM fiber organization in the centrum semovale. Crossing fibers are observed at the intersection between WM tracts. Colors indicate direction: red (R/L); green (A/P); blue (S/I).

V. Conclusion

The data presented here demonstrate that HYDI is a promising method for simultaneous acquisition of different types of diffusion image information. Work still needs to be done to validate and compare with other diffusion imaging methods. Further optimization of the encoding scheme may further improve the accuracy or enhance specific features of the diffusion data. For example, the resolution and quality of the ODF may be achieved by increasing the number of measurements in the outer shell and reducing the number of measurements in the inner shells. Alternatively, improved DTI measurements may be achieved by increasing the measurements in the inner shells.

Acknowledgment

The authors are grateful for discussions and assistance from Mariana Lazar, Jee Eun Lee, Ron Fisher, Terry Oakes, Aaron Field, John Carew and Guan Koay.

References

[1] Basser PJ et al. Estimation of the effective self-DT from the NMR spin echo. J Magn Reson B. 1994;103:247-54.

[2] Mulkern RV et al. Multi-component apparent diffusion coefficients in human brain. NMR Biomed. 1999;12:51-62.

[3] Niendorf T et al. Biexponential diffusion attenuation in various states of brain tissue... MRM 1996;36(6):847-57.

[4] Alexander AL et al. Analysis of partial volume effects in diffusion-tensor MRI. MRM 2001;45(5):770-80.

[5] Callaghan PT. Principles of Magnetic Resonance Microscopy. Oxford University Press. (1994).

[6] Wedeen VJ et al. Mapping complex tissue architecture with diffusion spectrum MRI. MRM 2005;54(6):1377-86.

[7] Alexander DC et al. Detection and modeling of non-Gaussian ADC profiles... MRM 2002;48(2):331-40.

[8] Frank LR. Characterization of anisotropy in high angular resolution DW MRI. MRM 2002;47(6):1083-99.

[9] Liu C et al. Characterizing non-Gaussian diffusion by using generalized diffusion tensors. MRM 2004;51:924-37.

[10] Ozarslan E, Mareci TH. Generalized diffusion tensor imaging... MRM 2003;50(5):955-65.

[11] Tuch DS. Q-ball imaging. MRM 2004;52(6):1358-72.

[12] Assaf Y et al. High b-value q-space analyzed DW MRI: application to multiple sclerosis. MRM 2002;47:115-26.